

# Surface-Enhanced Raman Scattering and Theoretical Studies of the C-Terminal Peptide of the $\beta$ -Subunit Human Chorionic Gonadotropin Without Linked Carbohydrates

A. E. Aliaga,<sup>1</sup> T. Aguayo,<sup>1</sup> C. Garrido,<sup>1</sup> E. Clavijo,<sup>1</sup> E. Hevia,<sup>2</sup> J. S. Gómez-Jeria,<sup>1</sup> P. Leyton,<sup>3</sup> M. M. Campos-Vallette,<sup>1</sup> S. Sanchez-Cortes<sup>4</sup>

<sup>1</sup> Laboratorio de Espectroscopía Molecular, Facultad de Ciencias, Universidad de Chile, PO Box 653, Santiago, Chile

<sup>2</sup> GrupoBios S.A. Av. Zañartu 1482, Ñuñoa, Santiago, Chile

<sup>3</sup> Departamento de Ciencias Químicas, Facultad de Ecología y Recursos Naturales, Universidad Andrés Bello (UNAB), Los Fresnos 52, Viña del Mar, Chile

<sup>4</sup> Instituto de Estructura de la Materia, CSIC, Serrano 121, 28006 Madrid, Spain

Received 1 June 2010; revised 10 August 2010; accepted 8 September 2010

Published online 24 September 2010 in Wiley Online Library (wileyonlinelibrary.com). DOI 10.1002/bip.21542

## ABSTRACT:

Raman and surface-enhanced Raman scattering (SERS) spectra of the synthetic carboxy terminal peptide of human chorionic gonadotropin  $\beta$ -subunit free of carbohydrate moieties (P37) are reported. The spectral analysis is performed on the basis of our reported Raman spectrum and SERS data of oligopeptides displaying selected amino acids sequences MRKDV, AEDRDA, and LRGISL. SERS samples of P37 were prepared by coating the solid peptide with metal colloids on a quartz slide. This treatment makes possible to obtain high spectral batch to batch reproducibility. Amino acids components of P37 display net charges and hydrophobic characteristics, which are related to particular structural aspects of the adsorbate–substrate interaction. The spectroscopic results

are supported by quantum chemical calculations performed by using extended Hückel theory method for a model of P37 interacting with an Ag surface. The P37–metal interaction is driven by positively charged fragments of selected amino acids, mainly threonine 109, lysine 122, and arginine in positions 114 and 133. Data here reported intend to contribute to the knowledge about the antigen–antibody interaction and to the drugs delivery research area. © 2010 Wiley Periodicals, Inc. *Biopolymers* 95: 135–143, 2011.

**Keywords:** Raman; surface-enhanced Raman scattering; carboxy terminal peptide of  $\beta$ -subunit of human chorionic gonadotropin; hCG $\beta$ -CTP; oligopeptides MRKDV, AEDRDA, and LRGISL; theoretical calculations

This article was originally published online as an accepted preprint. The “Published Online” date corresponds to the preprint version. You can request a copy of the preprint by emailing the *Biopolymers* editorial office at [biopolymers@wiley.com](mailto:biopolymers@wiley.com)

Correspondence to: M. M. Campos-Vallette; e-mail: [facien05@uchile.cl](mailto:facien05@uchile.cl)

Contract grant sponsor: CSIC-CONICYT

Contract grant number: 2007-145

Contract grant sponsors: Fondecyt

Contract grant number: 1070078, 1085124, and 1090074

Contract grant sponsors: Ministerio de Educación y Ciencia of Spain

Contract grant number: FIS2007-63065

Contract grant sponsors: Comunidad de Madrid

Contract grant number: S2009/TIC-1476 MICROSERES II

Contract grant sponsors: Doctoral Fellowship CONICYT (to A.E.A.)

Contract grant number: AT-24090050 (to A.E.A.)

© 2010 Wiley Periodicals, Inc.

## INTRODUCTION

Raman spectroscopy could afford important information about the mechanism of the aggregation undergone by peptides in aqueous solutions or when interacting with biological molecules. However, the application of this technique is highly limited by the large fluorescence emission of the biologic materials. These

drawbacks can be overcome when using metal nanoparticles (NPs) to partially quench the fluorescence emission and to enhance the Raman spectrum signals by surface-enhanced Raman scattering (SERS). NPs irradiated with a visible light of appropriate wavelength can induce a great intensification of the electromagnetic field on the surface through localized surface plasmon resonance, which consequently leads to a great enhancement of Raman signal from molecules adsorbed on NPs.<sup>1,2</sup> SERS has been an active research area with important applications ranging from surface chemistry to biological chemistry and biomedical analysis. Biosensors are intrinsically associated with peptide–metal NP systems.<sup>3–5</sup> The peptide–metal NP interaction also has important consequences on the optical properties of the NPs themselves. SERS of many amino acids, peptides, and proteins acquired with various SERS active substrates have been reported.

Recent results on the application of SERS to peptides have been published by Podstawka and Proniewicz,<sup>6</sup> who compared the adsorption behavior of bombesin (pGlu-Gln-Arg-Leu-Gly-Asn-Gln-Trp-Ala-Val-Gly-His-Leu-Met-NH<sub>2</sub>) and five bombesin-related peptides in silver colloidal solution. The peptide–metal interaction is mainly verified through the pyrrole ring of tryptophan and the aromatic ring of the phenylalanine components. They also infer a weak interaction through particular skeletal fragments of the peptidic chain. These results are slightly modified in the series of peptides. Differences in organization and orientation of the peptides on the metal surface by changing the silver colloidal surface by a silver electrode surface were inferred. SERS results by Di Foggia et al.<sup>7</sup> indicate that for four alternating polar/non-polar peptides derived from the self-assembling peptide EAK-16 (Ac-Ala-Glu-Ala-Lys-Ala-Glu-Ala-Lys-Ala-Glu-Ala-Gly-Ala-Glu-Ala-Lys-NH<sub>2</sub>) the interactions with TiO<sub>2</sub> mainly take place through carboxylate groups and that the self-assembled structure on the metal surface is predominantly a  $\beta$ -sheet. Mitchell et al.<sup>8</sup> used statistical analysis methods for the peptide detection by SERS. Wei et al.<sup>9</sup> registered the SERS spectra of three cysteine (Cys)-containing aromatic peptides and penetratin, bound to nanoshell substrates. It is concluded that the aromatic amino acid residues provide the dominant features in the SERS and Raman spectra. Seballos et al.<sup>10</sup> concluded from SERS spectra of several peptides composed by different combinations of proline, tryptophan, and tyrosine that the binding with a silver surface occurs through both the carboxylic end and the aromatic amino acids moieties.

Infrared techniques polarization modulation-reflection absorption infrared spectroscopy and attenuated total reflectance allowed to propose that the peptide  $\gamma$ -glutathione ( $\gamma$ -Gln-Cys-Gly) interacts with Au through the cysteine thiol group in water solution, and through the glycine carboxylate in ethanol.<sup>11</sup> A reflection absorption infrared spectroscopic

study on Ag was performed by Itoh et al.,<sup>12</sup> for Langmuir–Blodgett films of the palmitoyl-ornithine and palmitoyl-lysine peptides. Authors concluded on a particular organization of the peptides on the surface.

The usefulness of the SERS protocol will be highly dependent on the nature of the oligopeptide, in terms of length and sequence. The length and the sequence are important factors related with the three-dimensional conformation of the oligopeptide, which in turn, determines the accessibility of the molecules and the adsorption on a metal surface. On the other hand, the residual electrostatic charge, the hydrophilicity, and the existence of side chains containing chemical groups, which manifest a high affinity to the metal surface are key factors, which will determine the interaction strength of the oligopeptide with a metal surface.

Moreover, the interaction of peptides and oligopeptides with metal surfaces can occur through different mechanisms: (a) electrostatic interaction between positive charges in the oligopeptide and the negative residual charges existing on the metal surface, (b) coordination complexes formed between very active groups, such as -SH, -COO<sup>-</sup>, imidazol in histidine (His),<sup>13</sup> indole in tryptophan (Trp),<sup>14</sup> and surface metal atoms. Besides, the intermolecular interactions between oligopeptides should be considered. In this sense, the hydrophobic interactions between nonpolar amino acids residues in the oligopeptides also play an important role in both the three-dimensional conformation and the adsorption on the metal. Recent SERS results in our research group dealt with the oligopeptides MRKDV, ADEDRDA, and LGRGISL<sup>15</sup>; these oligopeptides display different net charges and hydrophobic characteristics, which were related to particular structural aspects of the adsorbate–substrate interaction. In all cases, the SERS spectra display signals coming from the guanidinium moiety of the arginine amino acid (R), which induces the orientation of the peptides on the metal surface. These spectroscopic results were supported by quantum chemical calculations.

In this frame, the aim of this contribution deals with the vibrational study of the synthetic carboxy terminal peptide (109–145, CTP) of human chorionic gonadotropin (hCG) free of carbohydrate moieties (P37 polypeptide) by SERS spectroscopy. Different spectral behavior of P37 respect to the already studied oligopeptides is expected. In fact, residues close to the probable metal-interacting molecular fragments and general physicochemical characteristics and size of P37 are different respect to the oligopeptides.

The hCG belongs to the glycoprotein hormone family, which includes luteinizing hormone (LH), follicle-stimulating hormone, and thyroid-stimulating hormone.<sup>16</sup> These hormones are formed by two subunits ( $\alpha$  and  $\beta$ ). The  $\alpha$ -subunit is common to all of them, whereas  $\beta$ , and despite the high

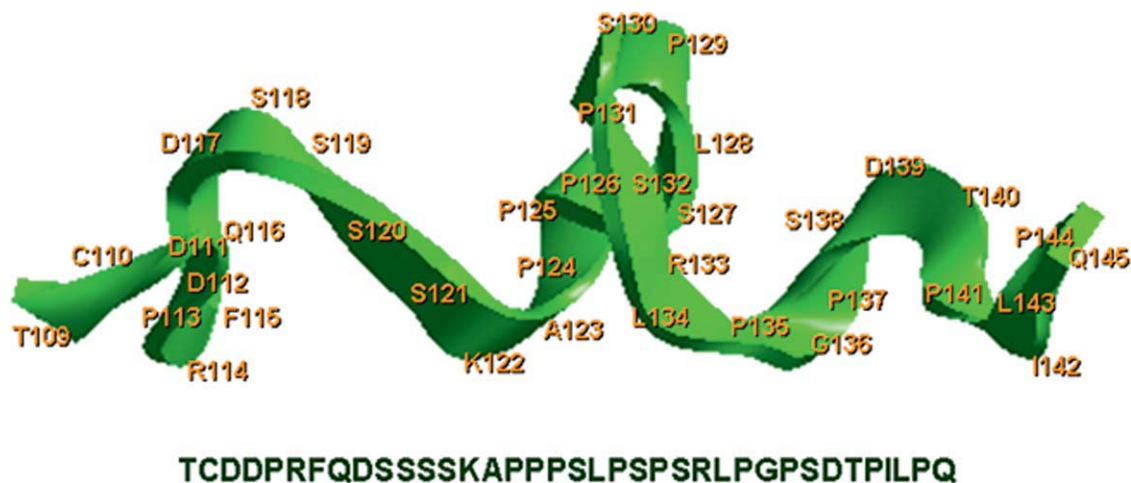


**FIGURE 1** Secondary structure and amino acid sequence of hCG $\beta$ -CTP without linked carbohydrates (P37 polypeptide). Molecular mechanic optimized geometry of P37 polypeptide.

degree of homology between them, presents differences that confer specificity. Thus, the first 110 amino acids of hCG $\beta$  ( $\beta$ -subunit of hCG) have a 85% homology with LH $\beta$  ( $\beta$ -subunit of LH), explaining why the majority of the antibodies against LH also recognize  $\beta$ hCG. However, the carboxy terminal end of hCG $\beta$  is unique; therefore, antibodies directed against this peptide are specific for hCG (do not recognize other hormones). Technology based on hCG $\beta$ -CTP not only has application in the diagnosis, because it is unique to hCG, but could also have an application in the development of a contraceptive vaccine.<sup>17,18</sup> The consequences of the substitution of arginine (68) of hCG $\beta$  with glutamic acid (R68E) are structurally relevant: in fact, the substitution profoundly reduces the cross-reactivity while refocusing the immune response to hCG $\beta$ -CTP. Berger et al.<sup>19</sup> studied the importance of carbohydrate moieties of hCG for epitope assembly. Two poorly immunogenic epitopes are located on the hCG $\beta$  113–116 and 137–144; the first involves the arginine residue surrounded by neutral and negative-charged amino acids, and the second displays carbohydrate moieties on the serine residue. Two antigenic regions hCG $\beta$  20–25 and hCG $\beta$  68–77 free of carbohydrate moieties on the natural polypeptide involve the lysine and arginine residues, respectively.

On the basis of the SERS data, we intend to determine the influence of the individual amino acids or in a sequence, the hydrophobicity and charge of the synthetic peptide, and the NPs interface characteristics, on the adsorption of the peptide on metal surfaces. To complete the analysis of the SERS experiments, a theoretical study based on the extended Hückel Theory (EHT) method for a simplified molecular model for the peptide surface interaction is proposed. The general methodology is similar to that used for oligopeptides in a previous work<sup>15</sup> but for a quite structurally different peptide.

## MATERIALS AND METHODS

### Samples

Water-soluble synthetic peptide from New England Peptide of analytical grade carboxy terminal polypeptide of hCG $\beta$ -CTP free of carbohydrates at serine in positions 121, 127, 132, and 138 (P37 polypeptide) was supplied by GrupoBios S.A (Figure 1). The amino acid sequence of P37 is H<sub>2</sub>N-TCDDPRFQDSSSSKAPPPSLPSPSRLPGPSDTPILPQ-OH; the molecular weight is 3876 g/mol. Stock solutions of the peptide in water were prepared to a final concentration of 10<sup>-5</sup>M. Aqueous stock solutions of the compound were prepared in nanopure water.

### Preparation of Silver NPs

Silver NPs (AgNPs) were prepared by chemical reduction of silver nitrate with both trisodium citrate (AgNPs-cit) and hydroxylamine hydrochloride (AgNPs-hyd).<sup>20</sup> The resulting colloids display a final pH of 5.5 and near 7, respectively. The aqueous solutions used for the AgNPs formation were prepared by using triply distilled water. Colloids showed a milky grey color.

### Preparation of Raman and SERS Samples

Several drops of aqueous 10<sup>-5</sup>M peptide solution were deposited onto a quartz slide. Solution samples were dried at room temperature. The Raman spectrum of the solid was obtained from several evaporations of the solution. The colloidal AgNPs-cit solution was dropped onto the P37 solid obtained from evaporating one drop of the solution. Room temperature dried sample was used for the SERS measurements.

### Instrumentation

The SERS spectrum of the peptide was measured with a Renishaw micro-Raman system (RM2000) using as excitation the 514 and 785 nm laser lines. Plasmon resonant effects were observed using the 514 nm laser line. However, a rapid heating is observed avoiding scan reproducible spectra. The Raman and SERS reproducible spectral

data were obtained by using the 785 nm laser line. A lower spectral intensity compared with the spectra using 514 nm was observed. The instrument was equipped with a Leica microscope, and an electrically cooled CCD camera. The signal was calibrated by using the  $520\text{ cm}^{-1}$  line of a Si wafer and a  $\times 50$  objective. The laser power on the sample was 2 mW. The resolution was set to  $4\text{ cm}^{-1}$ , and 5–20 scans of 10 s each were averaged. Spectra were recorded in the  $200\text{--}4000\text{ cm}^{-1}$  region to observe both the Raman and SERS spectra. The spectral scanning conditions are chosen to avoid sample degradation.

### Spectral Reproducibility

No reproducible SERS spectra were obtained by using the traditional way, that is, by addition of the sample solution to the colloidal suspension or the inverse. The SERS reproducible spectra from batch to batch were obtained by adding the colloidal AgNPs solution onto the dried analyte sample.

### Molecular Models and Calculations

To complete the analysis of the SERS experiments, a theoretical study was performed. A simplified molecular model for the analyte–metal surface interaction is proposed. The silver (Ag) atom's surface was slightly different to the one used in our previous studies.<sup>21–23</sup> Briefly, a face centered-cubic structure with  $a = 0.408\text{ nm}$  was built and trimmed to get a planar single layer composed of 356 silver atoms. This is to prevent that any part of the polypeptide could interact with the border of the metallic layer.

The polypeptide was studied in its full ionized state. Because of the experimental conditions, molecular mechanics was used to optimize the polypeptide–Ag geometry, keeping the Ag layer geometry constant for each case. Several different starting geometries for the polypeptide–Ag layer system were tested; all of them produced the

final geometry employed here. EHT was used to calculate the wave function of the Ag layer, the polypeptide as an isolated system, and the polypeptide–metal surface system (Figure 2). EHT calculations produce qualitative or semiquantitative descriptions of molecular orbital and electronic properties.<sup>24</sup> EHT is the simplest semiempirical method, but it may be regarded as a method of simulating Hartree–Fock (HF) calculations by guessing the elements of the HF Hamiltonian matrix through the use of the Wolfsberg–Helmholtz approximation.<sup>25</sup> Also, it was shown that within the Hartree–Fock–Rüdenberg picture, EHT is compatible with the nonempirical HF method in Roothaan's form.<sup>26,27</sup> These facts explain why EHT turned out to be qualitatively successful. The Hyperchem program was used.<sup>28</sup> The combination of EHT with molecular mechanics was able to give, for example, a qualitative explanation of our previous SERS works in oligopeptides,<sup>15</sup> nanotubes,<sup>21</sup> tryptophan,<sup>22</sup> lysine,<sup>23</sup> humic acids,<sup>29</sup> and arginine<sup>30</sup> interacting with Ag surfaces.

## RESULTS AND DISCUSSION

### Physicochemical Properties of the P37 Polypeptide

Table I contains physical and physicochemical properties of the studied peptide. The zeta potential of AgNPs is negative in a large pH range.<sup>31</sup> From the net charge values and hydrophobic or hydrophilic characteristics was possible to infer about the peptide–metal interaction for AEDRDA, LGRGISL, and MRKDV.<sup>15</sup> SERS spectra were observed for the three peptides by coating them with AgNPs. Spectra are dominated by signals coming from the amino acid residues, mainly Arg (R) in MRKDV; the other amino acid compo-

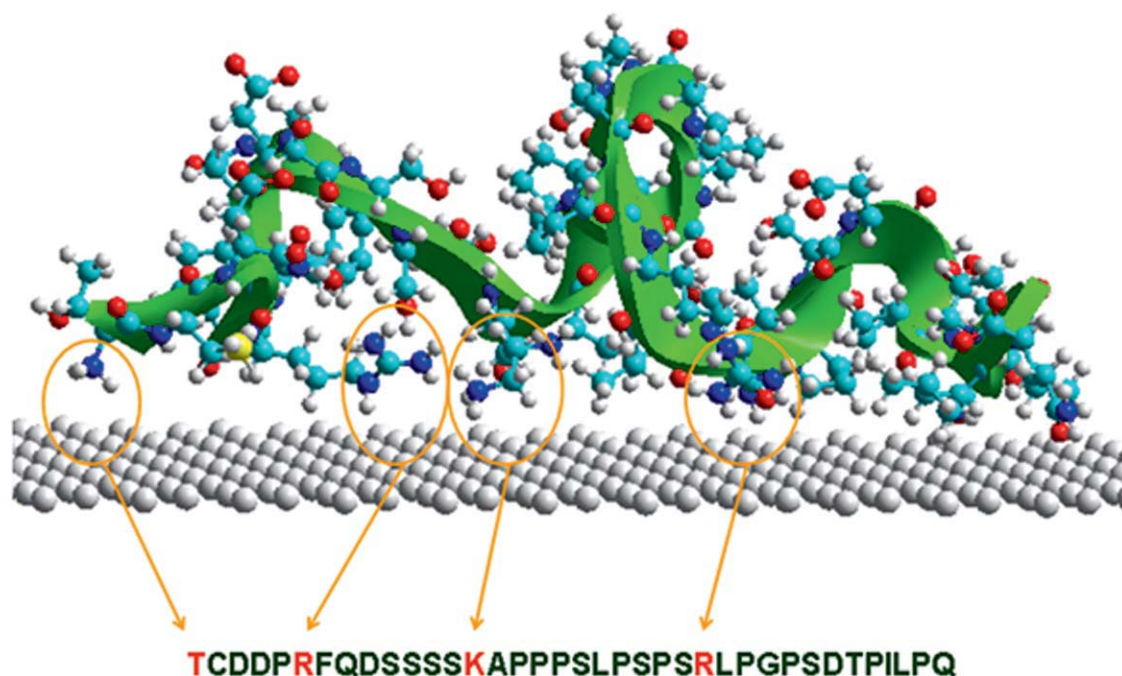


FIGURE 2 Predicted molecular model for the P37–Ag interaction.



**Table I** Properties of the Carboxy Terminal Polypeptide of hCG $\beta$ -CTP Free of Carbohydrate Moieties (P37); Structural Amino Acid Components, Hydrophilicity Index,<sup>45</sup> and net charge<sup>46</sup>

Amino Acids Position	Peptide	Hydrophilicity Index	Net Charge <sup>a</sup>
	P37	0.3	-1
109	Thr T	-0.4	0
	Cys C	-1.0	0
	Asp D	3.0	-1
	Asp D	3.0	-1
	Pro P	0.0	0
114	Arg R	3.0	+1
115	Phe F	-2.5	0
	Gln Q	0.2	0
	Asp D	3.0	-1
	Ser S	0.3	0
	Ser S	0.3	0
120	Ser S	0.3	0
	Ser S	0.3	0
122	Lys K	3.0	+1
	Ala A	-0.5	0
	Pro P	0.0	0
125	Pro P	0.0	0
	Pro P	0.0	0
	Ser S	0.3	0
	Leu L	-1.8	0
	Pro P	0.0	0
130	Ser S	0.3	0
	Pro P	0.0	0
	Ser S	0.3	0
133	Arg R	3.0	+1
	Leu L	-1.8	0
135	Pro P	0.0	0
	Gly G	0.0	0
	Pro P	0.0	0
	Ser S	0.3	0
	Asp D	3.0	-1
140	Thr T	-0.4	0
	Pro P	0.0	0
	Ile I	-1.8	0
	Leu L	-1.8	0
	Pro P	0.0	0
145	Gln Q	0.2	0

<sup>a</sup> Calculated at pH 7.

nents in ADEDRDA and LGRGISL are also expressed, being their aliphatic and carboxylic fragments responsible of the most intense spectral signals. The amino acid structural characteristic of the Arg moiety rather than its position in the context of a polypeptidic sequence plays an important role in the peptide-AgNPs interaction.

On the basis of the experimental and theoretical data of the reference peptides<sup>15</sup> and the partial and net charge and hydrophilicity index of P37, we could infer about both the possibil-

ity that this peptide displays a SERS spectrum and that the peptide metal interaction, if occurs, takes place through the positively charged amino acid moieties. P37 displayed a net charge equal to -1 at pH 7. The average hydrophilicity is 0.3, and the ratio of hydrophilic residues/total number of residues is 46%. Physicochemical data in Table I suggest a nonevident adsorbate-substrate interaction. However, we could expect that at least three fragments of the peptide P37 interact with the metal surface through the positive-charged fragments of arginine (R) in positions 114 and 133 (Arg-114 and Arg-133), and lysine (K) in position 122 (Lys-122), respectively. Numbering is in concordance with description given for the natural polypeptide.<sup>16,19</sup> This proposition could be modified by a detailed analysis of the neighboring amino acid characteristics. In the first case (DPRFQ segment), Arg-114 is surrounded by neutral and negative charges of hydrophilic amino acids, which make improbable the interaction with the metal. This situation is less drastic in the case of Lys-122 (SSKAP) and Arg-133 (PSRLP), where the closest amino acids are neutral and low charged, and some of them, Ala-123 and Leu-134, displaying rather hydrophobic characteristics (Table I).

These hypotheses were confirmed. In fact, it was possible to obtain a net SERS spectrum for P37. The high negative value of the zeta potential in the case of AgNPs-cit accounts for the absence of the carboxylate bands and the intensification of particular spectral signals of the positively charged lysine and arginine residues.

### Raman and SERS Spectra

The analysis of the Raman spectrum of P37 was performed on the basis of data concerning our published results (Ref. 15 and references Therein) and others' related molecules.<sup>32-43</sup> Table II contains the proposed bands assignment. There are bands observed only in the Raman spectrum of the peptide, which are ascribed to vibrational modes involving the identical amino acidic functions in all the amino acids: 1678 ( $\nu$ C=O,  $\delta$ NH amide I), 1327 ( $\nu$ CN, CH def), 1103 ( $\delta$ NH<sub>3</sub><sup>+</sup>), 725 ( $\rho$ CH<sub>2</sub>, COO<sup>-</sup> def), and 406 cm<sup>-1</sup> ( $\delta$ CN). Other bands are characteristics of phenylalanine (1007 cm<sup>-1</sup>) and aspartic acid (882 cm<sup>-1</sup>).

When it was possible to obtain a SERS spectrum in colloidal AgNPs solution for the peptide, a unique and reproducible spectrum was not achieved. The reproducible SERS spectrum of the peptide in solid, that is, the analyte coated by the metal nanostructures, was succeeding. The spectral analysis of the SERS spectra was performed on the basis of previous and own Raman and SERS band assignments for most of the amino acid residues of the present peptide.<sup>32-36</sup> The Raman and SERS spectra of the peptide are displayed in Figure 3, whereas the SERS of lysine and arginine are displayed in Figure 4.

**Table II Raman and SERS Frequencies ( $\text{cm}^{-1}$ ) of P37 and the Most Probable Band Assignment; SERS Frequencies of Lysine<sup>23</sup> and Arginine<sup>30</sup>**

Raman P37	SERS P37	Assignment <sup>a</sup>	SERS Lysine	SERS Arginine
1678	1710	Amide I $\nu\text{C}=\text{O} + \delta\text{NH}$		
	1629		1639	1653
	1578	$\delta\text{NH}, \delta\text{NH}_3^+, \nu\text{COO}^-$		1569
				1479
1461	1457	K	1447	1444
			1402	1412
	1381	A $\nu_s\text{COO}^-$		
	1360	S	1355	1355
1339	1337	L		1325
1327		$\nu\text{CN}, \text{CH def}$		
1257	1273	L	1280	
1206	1196	K	1207	
		R		1169
1131	1112	S	1127	
1103		$\delta\text{NH}_3^+$		
1054	1051	R	1032	1088
1007		F		
	998	R		978
924	954	R		934
882		D		
	867	L		
835	821	R	847	839
794	795	S	796	781
	770	A	773	
725		$\rho\text{CH}_2, \text{COO}^- \text{ def}$		
	672	S		665
	652	K		
	611	A		611
600	594	A		
	563	$\rho\text{CO}, \omega\text{NH}_2, \text{K}$		535
484	460	K	460	
406		$\delta\text{CN}$		

<sup>a</sup> Most probable assignment expressed mainly in terms of the amino acid symbol: R, arginine; K, lysine; D, aspartic acid; L, leucine; G, glycine; I, isoleucine; S, serine; A, alanine. For the specific normal modes involved in the vibrations, please see Refs. 33 and 34.

Table II contains the most probable assignment expressed in terms of the amino acid symbol. Details of the corresponding normal modes are given by Stewart and Fredericks.<sup>33,34</sup>

A broad and multiple band is observed around  $1600 \text{ cm}^{-1}$  with maxima at  $1629 \text{ cm}^{-1}$  and  $1578 \text{ cm}^{-1}$  in the SERS spectrum of P37. These bands are attributed to carboxylate stretching and NH and  $\text{NH}_3^+$  deformation modes. The  $\text{NH}_3^+$  deformation bands should correspond to the Thr-109, placed in the amino-terminal part of the peptide (Figure 2), and Lys-122 amino acids. The existence of such bands is the first evidence of the interaction of those amino acid fragments with the metal surface.

The following SERS spectral discussion is performed in terms of both the general spectral features and the spectral behavior of amino acid sequences involving the arginine and lysine residues.

### PSRLP (131–135) Segment

The arginine SERS bands observed at 1051, 998, 954, and  $821 \text{ cm}^{-1}$  are ascribed to vibrations of the guanidinium moiety. Leucine (L) bands are observed at 1337, 1273, and  $867 \text{ cm}^{-1}$ . Serine (S) bands are identified at 1360, 1112, 795, and  $672 \text{ cm}^{-1}$ . Proline (P) signals are not observed. This spectral behavior suggests that at least the SRL fragment interacts with the metal surface. Thus, the discussed Arg signals come from the amino acid residue in position 133.

### SSKAP (120–124) Segment

Lysine (K) bands are expected at 1457, 1196, 652, 563, and  $460 \text{ cm}^{-1}$ . The alanine (A) bands are assigned to the very weak bands at 1381, 770, 611, and  $594 \text{ cm}^{-1}$ . This spectral situation plus the presence of the serine bands already described in segment PSRLP indicates that the lysine residue

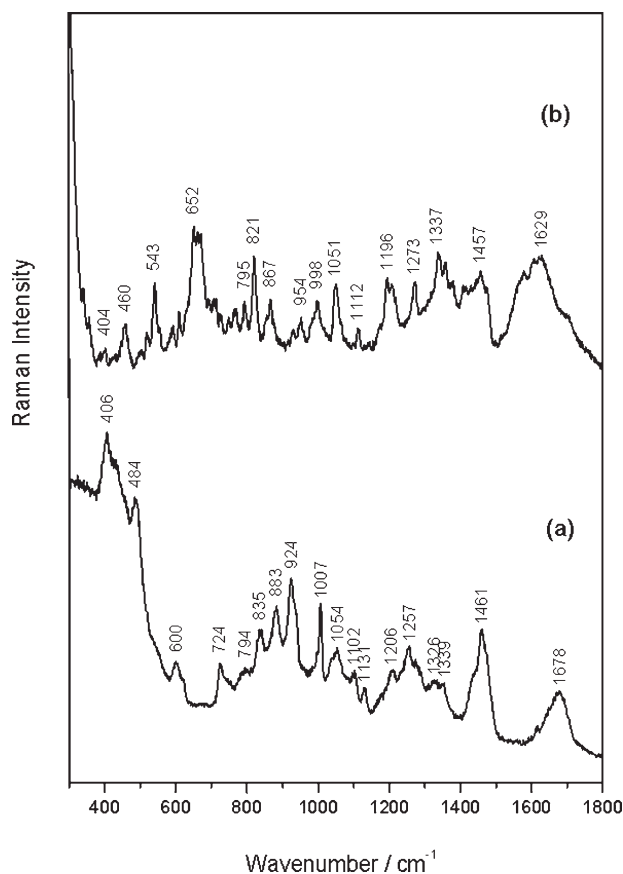


FIGURE 3 (a) Raman and (b) smoothed SERS spectra of P37.

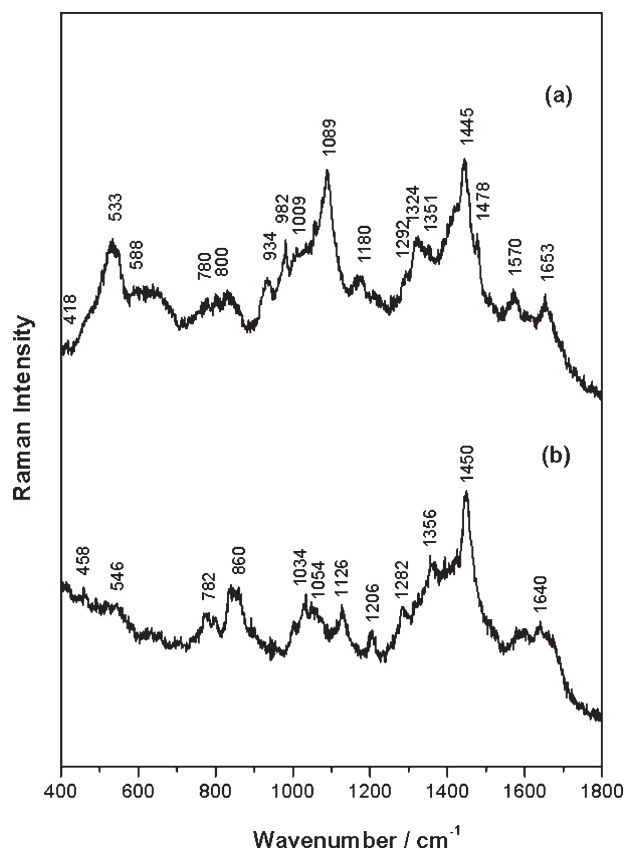


FIGURE 4 SERS of (a) arginine<sup>30</sup> and (b) lysine.<sup>23</sup>

in position 122 drives the orientation of this fragment of the peptide to the metal surface.

### DPRFQ (112–116) Segment

The phenylalanine (F) characteristic intense SERS band normally observed close to  $1007\text{ cm}^{-1}$  is not present. SERS proline (P) bands expected near  $1170$  and  $1080\text{ cm}^{-1}$  and others from the glutamine (Q) near  $1430$ ,  $1400$ , and  $1070\text{ cm}^{-1}$  are also not observed. The aspartic acid (D) bands are not observed excepting that at  $882\text{ cm}^{-1}$ , appearing only in the Raman spectrum of the peptide. These results and those of the already discussed segments suggest that Arg-114 is probably far from the metal surface.

The most relevant frequency shifting between Raman and SERS spectra in Table II mainly concern vibrational modes involving residues interacting with the metal surface. Thus, the most probable orientation of the peptide on the metal surface is governed, besides the Thr-109 residue, by the fragments where the Arg and Lys residues are surrounded by positive or neutral amino acids displaying the lower hydrophilic index.

The SERS spectral profile of the peptide in the amide I ( $1675$ – $1655\text{ cm}^{-1}$ ) and III ( $1280$ – $1230\text{ cm}^{-1}$ ) regions along

with normally observed skeletal bands in the  $960$ – $900\text{ cm}^{-1}$  region is not characteristic of any clear conformational structure. A rather disordered conformation is induced by the high number of proline residues (10 residues) existing in P37, which act as structural disruptors of the sequence.<sup>44</sup>

### Theoretical Aspects

**P37–Metal Interaction.** For the isolated Ag layer, the highest occupied molecular orbital (HOMO)–lowest unoccupied molecular orbital gap is  $0.03\text{ eV}$ , and the occupied and empty molecular orbitals are highly packed, indicating that the proposed surface structure is an acceptable model of a metallic Ag cluster. The final polypeptide–Ag surface system is shown in Figure 2. The positive charged groups closest to the silver surface are  $\text{NH}_3^+$  of Thr-109 and Lys-122, and the guanidinium groups of Arg in positions 114 and 133. The N atom of the  $\text{NH}_3^+$  group of Thr-109 is located at  $3.65\text{ \AA}$  from the surface. The N atom of the  $\text{NH}_3^+$  group of Lys-122 is at about  $2.9\text{ \AA}$  from the silver surface. In the guanidinium group of Arg-114, one of the N atoms is at about  $3.8\text{ \AA}$  from the surface and the N atom bonded to the alkyl chain is at about  $3.3\text{ \AA}$ . In Arg-133, one of the N atoms is at about  $4.0\text{ \AA}$  of the silver surface, whereas the other is at about  $3.3\text{ \AA}$ . All these groups are located close to the Ag surface in which the electronic density of the first two HOMO and HOMO-1 of the surface are zero. This is a suitable position for a guanidinium group, which has an overall positive charge but with two N atoms carrying negative net charges because it minimizes the electron–electron repulsion. Because the empty  $\pi$  molecular orbitals of the two arginine groups are perpendicular to the HOMO of the Ag layer, they do not overlap. Therefore, no charge transfer is expected between the polypeptide and the Ag layer.

Two carbonyl oxygen atoms of Ile-142 and Gln-145 are located in the  $3.1$ – $3.3\text{ \AA}$  range from the silver surface. They are close to surface areas where the electronic density of the Ag layer lowest unoccupied molecular orbital is very low, precluding, therefore, a charge transfer between these moieties. Thus, these results strongly suggest that the polypeptide–silver layer interaction is of an electrostatic type, and that this interaction takes place predominantly through the Arg-133 and Lys-122 residues, together with the amino terminal Thr-109 amino acid (Figure 2).

### CONCLUSIONS

The analysis of the net charge values and hydrophilic characteristics of the synthetic CTP of hCG $\beta$ -CTP without O-linked carbohydrate moieties at serine in positions 121, 127,

132, and 138 (P37) makes possible to infer about the SERS activity, and then to propose an idea about the way how this polypeptide could interact with a metal surface. Propositions are confirmed by experimental SERS data. SERS spectra were observed for the polypeptide by coating it with AgNPs; this innovation also allows obtain reproducible spectra. The SERS spectrum of P37 is dominated by signals coming from the amino acid residues, mainly arginine (R) in position 133 and lysine (K) in position 122; other amino acid components leucine (L), alanine (A), and serine (S), surrounding arginine and lysine, are also expressed. The amino acid chemical characteristics of the arginine and lysine residues and their position in the context of a determined peptide fragment play an important role in the polypeptide-AgNPs interaction. Moreover, it is expected that post-translational modifications on determined serine residues with carbohydrates for instance, could modify the peptide metal interaction, involving other molecular segments. Theoretical results confirm the inductive effect imposed by the guanidinium moiety of arginine and the ammonium group of lysine and threonine. The proposed structural model for the polypeptide Ag surface system suggests that the P37-Ag interaction is almost totally electrostatic. The SERS spectral profile of the polypeptide in the amide I and III regions along with the skeletal bands do not allow propose a definitive conformational structure under the present experimental conditions.

## REFERENCES

- Moskovits, M. *Rev Mod Phys* 1985, 57, 783–826.
- Aroca, R. *Surface-Enhanced Vibrational Spectroscopy*; John Wiley & Sons: Chichester, 2006.
- Ramanathan, S.; Ensor, M.; Daunert, S. *Trends Biotechnol* 1997, 15, 500–506.
- Marvin, J. S.; Hellinga, H. W. *Proc Natl Acad Sci USA* 2001, 98, 4955–4960.
- Bontidean, I.; Kumar, A.; Csoregi, E.; Galaev, I. Y.; Mattiasson, B. *Angew Chem Int Ed* 2001, 40, 2676–2678.
- Podstawka, E.; Proniewicz, L. M. *J Phys Chem B* 2009, 113, 4978–4985.
- Di Foggia, M.; Taddei, P.; Fagnano, C.; Torreggiani, A.; Dettin, M.; Sanchez-Cortes, S.; Tinti, A. *J Mol Struct* 2009, 120, 924–926.
- Mitchell, B. L.; Patwardhan, A. J.; Ngola, S. M.; Chan, S.; Sundararajan, N. *J Raman Spectrosc* 2008, 39, 380–388.
- Wei, F.; Zhang, D.; Halas, N. J.; Hartgerink, J. D. *J Phys Chem B* 2008, 112, 9158–9164.
- Seballos, L.; Richards, N.; Stevens, D. J.; Patel, M.; Kapitzky, L.; Lokey, S.; Millhauser, G.; Zhang, J. Z. *Chem Phys Lett* 2007, 447, 335–339.
- Bieri, M.; Burgi, T. *Langmuir* 2005, 21, 1354–1363.
- Itoh, K.; Ohe, C.; Tsurumaru, T.; Yasukawa, S.; Yamaguchi, T.; Kasuya, G. *Vib Spectrosc* 2002, 29, 197–203.
- Lim, J. K.; Kim, Y.; Lee, S. Y.; Joo, S.-W. *Spectrochim Acta A* 2008, 69, 286–289.
- Sarkar, J.; Chowdhury, J.; Ghosh, M.; De, R.; Talapatra, G. B. *J Phys Chem B* 2005, 109, 12861–12867.
- Garrido, C.; Aliaga, A. E.; Gomez-Jeria, J. S.; Clavijo, R. E.; Campos-Vallette, M. M.; Sanchez-Cortes, S. *J Raman Spectrosc* 2010, doi: 10.1002/jrs. 2583.
- Lapthorn, A. J.; Harris, D. C.; Littlejohn, A.; Lustbader, J. W.; Canfield, R. E.; Machin, K. J.; Morgan, F. J.; Isaacs, N. W. *Nature* 1994, 369, 455–461.
- Berber, P.; Sturgeon, C.; Bidart, J. M.; Paus, E.; Gerth, R.; Niang, M.; Bristow, A.; Birken, S.; Stenman, U. H. *Tumor Biol* 2002, 23, 1–38.
- Charrel-Dennis, M.; Terrazzini, N.; McBride, J. D.; Kaye, P.; Martensen, P. M.; Justesen, J.; Berger, P.; Lapthorn, A.; Kelly, C.; Roitt, I. M.; Delves, P. J.; Luna, T. *Mol Endocrinol* 2005, 19, 1803–1811.
- Berger, P.; Bidart, J. M.; Delves, P. S.; Dirnhofer, S.; Hoermann, R.; Issacs, N.; Jackson, A.; Klonisch, T.; Lapthorn, A.; Lund, T.; Mann, K.; Roitt, I.; Schwarz, S.; Wick, G. *Mol Cell Endocrinol* 1996, 125, 33–43.
- Leopold, N.; Lendl, B. *J Phys Chem B* 2003, 107, 5723–5727.
- Leyton, P.; Gómez-Jeria, J. S.; Sanchez-Cortes, S.; Domingo, C.; Campos-Vallette, M. M. *J Phys Chem B* 2006, 110, 6470–6474.
- Aliaga, A. E.; Osorio-Román, I.; Leyton, P.; Garrido, C.; Cárcamo, J.; Caniulef, C.; Célis, F.; Diaz-Fleming, G.; Clavijo, E.; Gómez-Jeria, J. S.; Campos-Vallette, M. M. *J Raman Spectrosc* 2009, 40, 164–169.
- Aliaga, A. E.; Osorio-Román, I.; Garrido, C.; Leyton, P.; Cárcamo, J.; Clavijo, E.; Gómez-Jeria, J. S.; Diaz-Fleming, G.; Campos-Vallette, M. M. *Vib Spectrosc* 2009, 50, 131–135.
- Gómez-Jeria, J. S. *J Comp Theor Nanosci* 2009, 6, 1361–1369.
- Boer, F. P.; Newton, M. D.; Lipscomb, W. N. *Proc Natl Acad Sci USA* 1964, 52, 890–893.
- Koch, W. *Int J Quantum Chem* 2000, 76, 148–160.
- Koch, W.; Frey, B.; Sanchez-Ruiz, J. F.; Scior, T. *Z Naturforsch A* 2003, 58, 756–784.
- HyperChem (TM); Hypercube, Inc.: Gainesville, FL, 2007.
- Leyton, P.; Córdova, I.; Lizama-Vergara, P. A.; Gómez-Jeria, J. S.; Aliaga, A. E.; Campos-Vallette, M. M.; Clavijo, E.; García-Ramos, J. V.; Sánchez-Cortés, S. *Vib Spectrosc* 2008, 46, 77–81.
- Aliaga, A. E.; Garrido, C.; Leyton, P.; Diaz-Fleming, G.; Clavijo, E.; Campos-Vallette, M. M.; Sanchez-Cortes, S. *Spectrochim Acta A: Mol Biomol Spectrosc* 2010, 76, 458–463.
- Alvarez-Puebla, R. A.; Arceo, E.; Goulet, P. J. G.; Garrido, J. J.; Aroca, R. F. *J Phys Chem B* 2005, 109, 3787–3792.
- Ngola, S. M.; Zhang, J.; Mitchell, B. L.; Sundararajan, N. *J Raman Spectrosc* 2008, 39, 611–617.
- Stewart, S.; Fredericks, P. M. *Spectrochim Acta A* 1999, 55, 1615–1640.
- Stewart, S.; Fredericks, P. M. *Spectrochim Acta A* 1999, 55, 1641–1660.
- Diaz-Fleming, G.; Finnerty, J. J.; Campos-Vallette, M. M.; Célis, F.; Aliaga, A. E.; Fredes, C.; Koch, R. *J Raman Spectrosc* 2009, 40, 632–638.
- DeGelder, J.; DeGussem, K.; Vandenaabeele, P.; Moens, L. *J Raman Spectrosc* 2007, 38, 1133–1147.
- Lin-Vien, D.; Colthup, N. B.; Fateley, W. G.; Graselli, J. G. *The Handbook of Infrared and Raman Characteristic Frequencies of Organic Molecules*, 1st ed.; Academic Press: Boston, MA, 1981.



38. Ramaswamy, S.; Rajaram, R. K.; Ramakrishnan, V. *J Raman Spectrosc* 2003, 34, 50–56.
39. Lima, R. J. C.; Freire, P. T. C.; Sasaki, J. M.; Melo, F. E. A.; Filho, J. M. *J Raman Spectrosc* 2002, 33, 625–630.
40. Zawadzki, H. J. *Trans Metal Chem* 2003, 28, 820–826.
41. DiCostanzo, L.; Flores, L. V.; Christianson, D. W. *Proteins: Struct Funct Bioinf* 2006, 65, 637–642.
42. Guerrini, L.; Izquierdo-Lorenzo, I.; Garcia-Ramos, J. V.; Domingo, C.; Sanchez-Cortes, S. *Phys Chem Chem Phys* 2009, 11, 7363–7371.
43. Arenas, J. E.; Castro, J. L.; Otero, J. C.; Marcos, J. I. *Biopolymers* 2001, 62, 241–248.
44. Jiang, P.; Xu, W.; Mu, Y. *PLoS Comput Biol* 2009, 5, e1000357.
45. Hoop, T. P.; Woods, K. R. *Proc Natl Acad Sci USA* 1981, 78, 3824.
46. Kyte, J.; Doolittle, R. F. *J Mol Biol* 1982, 157, 105.

*Reviewing Editor: C. Allen Bush*